

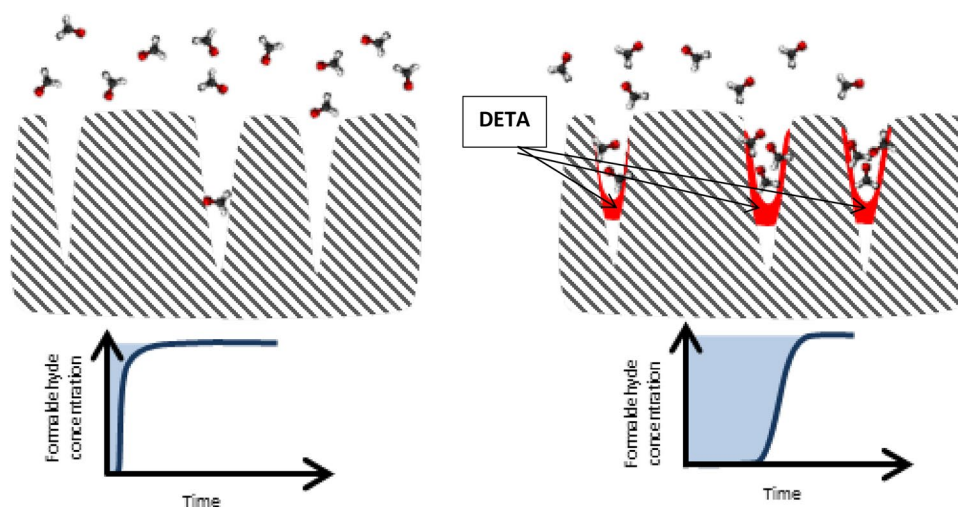
# Amine functionalized activated carbon fibers as effective structured adsorbents for formaldehyde removal

Guillaume B. Baur<sup>1</sup> · Jonathan Spring<sup>1</sup> · Lioubov Kiwi-Minsker<sup>1,2</sup> 

Received: 5 January 2018 / Revised: 10 September 2018 / Accepted: 15 September 2018 / Published online: 29 September 2018  
© Springer Science+Business Media, LLC, part of Springer Nature 2018

## Abstract

Activated carbon fibers (ACFs) with surface modified by a diethylene triamine (DETA) are synthesized for the abatement of formaldehyde in gas phase at low concentration. Adsorbents with several DETA loadings were tested and characterized. The amount of DETA deposited on the ACFs surface is shown to diminish the porosity. The influence of the DETA on the adsorption capacity towards formaldehyde is studied via dynamic adsorption experiments. The deposition of 20 wt.% DETA allowed ~100-fold increase of adsorption capacity as compared to original ACFs. A Schiff base reaction between the amine groups of DETA and formaldehyde was suggested as the adsorption mechanism. Adsorbent surface chemistry was shown to be more important than its microporous structure for efficient formaldehyde removal.



**Keywords** Activated carbon fibers · Surface modification · DETA · Formaldehyde removal

## 1 Introduction

Formaldehyde is a polar volatile organic compound (VOC) emitted by different industries such as refineries, ink plants or as by-product of incomplete combustion. It is known as a highly toxic anthropogenic pollutant leading to cancer (Hauptmann et al. 2004). World Health Office recommends a maximum concentration of 0.08 ppm to avoid its carcinogenic effects (WHO 2000). Therefore, the development of effective abatements methods for formaldehyde at very low concentration in the gas streams is warranted.

✉ Lioubov Kiwi-Minsker  
lioubov.kiwi-minsker@epfl.ch

<sup>1</sup> Group of Catalytic Reaction Engineering, Ecole Polytechnique Fédérale de Lausanne, EPFL-SB-ISIC-GGRC, Station 6, CH-1015 Lausanne, Switzerland

<sup>2</sup> Regional Technological Centre, Tver State University, Tver, Russian Federation 170100

Between the available methods of abatement, adsorption has been reported as the most suitable due to its simplicity, efficiency and economic viability (Lee et al. 2013). However, in the case of formaldehyde high removal efficiency at low concentration in air is particularly challenging to reach. Indeed its low boiling point (254 K) hinders pore condensation even within highly porous adsorbents (Pei and Zhang 2011). Moreover, its polarity reduces the chemical interactions with non-polar materials like activated carbon or high-porous polymers.

Nevertheless, several adsorbents used for formaldehyde abatement were shown effective like activated carbon with high content of functional hydrophilic groups (Boonamnuayvitaya et al. 2005) and large pore volume (Rong et al. 2003). The surface functionalization of zeolite (Kim et al. 2011), amorphous silica (Ewlad-Ahmed et al. 2012) and activated carbon (Tanada et al. 1999; Lee et al. 2013; Carter et al. 2011) by nitrogen-containing groups was reported to promote formaldehyde adsorption. Graphite oxide containing amino groups was also reported as an effective adsorbent (Matsuo et al. 2008). In line with the later results the deposition of hexamethylene diamine on activated carbon led to a significant increase of the adsorption capacity towards formaldehyde in gas phase (Ma et al. 2011).

In our previous publications (Baur et al. 2015c) activated carbon fibers (ACFs) were shown suitable adsorbents for toluene removal due to high specific surface area, large pore volume, absence of large pressure drop during the gas passage through the adsorbing bed and low mass transfer limitations (Singh et al. 2002). The effect of surface functionalities of ACFs on the adsorption of acetaldehyde at low concentrations (~80 ppmv) and short contact time (20 ms) has also been studied. It was shown that functional groups such as polar groups (Baur et al. 2015a) or nanoparticle of basic metal oxides (Baur et al. 2015b) can considerably increase the adsorption capacity via chemical interactions between the functional groups and the adsorbate.

In this study ACFs were surface-functionalized by amino-groups via the deposition of diethylene triamine (DETA) on fiber's surface. A chemical interaction of formaldehyde with DETA should insure its fast and irreversible adsorption. The deposition of immobilized liquid on a hollow fiber surface for toluene or acetone removal was already reported (Obuskovic et al. 2003). An increased performance was shown in terms of separation factor between the VOC vapor and the carrier gas.

The objectives of the present study were to develop a novel structured carbon based adsorbent by a deposition of DETA on the ACFs surface. The performance of the developed adsorbent towards formaldehyde removal at short contact time is evaluated by transient response method and the adsorbents are characterized by different physico-chemical technics (BET,  $\alpha_s$ -plot, TPD, SEM).

## 2 Experimental part

### 2.1 Material

ACFs provided by Kynol Europa GmbH (Hamburg, Germany) in the form of woven tissues were used as starting materials. The specific surface area (SSA) announced by the provider is ~2000 m<sup>2</sup> g<sup>-1</sup>. The ACFs are produced from novoloid phenolic precursor fibers by a one step process combining carbonization and chemical activation.

The ACFs were modified by deposition of a diethylenetriamine (DETA) (99% Sigma–Aldrich) via wetness impregnation. In a standard procedure, the ACFs the samples were air-dried at 373 K for 2 h and dipped into a solution of DETA in ethanol (> 99.8% Fluka). The concentrations were calculated using the ACFs wetness capacity to obtain several final DETA loadings (5–35 wt.%). The impregnated samples were then dried in ambient air to remove the ethanol.

### 2.2 Adsorbent characterization

The specific surface area (SSA) and pore size distribution (PSD) were determined by physical adsorption of N<sub>2</sub> at 77 K using a Sorptomatic 1990 (Carlo Erba Instruments). Prior to analysis, the samples were outgassed at 373 K for 2 h under vacuum (7·10<sup>-2</sup> bar). N<sub>2</sub> adsorption/desorption isotherms were recorded at 77 K over the relative pressure range of 0.0005 ≤ p/p<sub>0</sub> ≤ 0.98. The total pore volume and specific surface area were calculated using BET method.

Scanning electron microscopy (SEM) was carried out using a Carl Zeiss MERLIN FE-SEM equipped with two, annular and Everhart–Thornley secondary-electron (SE), detectors operated at an accelerating voltage of 5–30 keV with a beam current of 1.0–3.0 nA and using ZeissSmart-SEM software for data acquisition/manipulation.

### 2.3 Dynamic adsorption measurement

Before any measurements, the samples (20 ± 0.1 mg) were placed in the central part of the glass tubular reactor and outgassed at 373 K in a He flow (40 cm<sup>3</sup> min<sup>-1</sup>) for 30 min. The dynamic adsorption experiments were carried out at 298 ± 1 K with a gas flow rate of 300 cm<sup>3</sup>·min<sup>-1</sup> (linear velocity—0.5 m·s<sup>-1</sup>) regulated by mass flow controllers (EL-FLOW, Bronkhorst). The gaseous mixture containing 50 ppmv of formaldehyde in He is obtained from a gas generator (Flex-Stream, Kin-Tek). Ar tracer (2% v/v) in He was injected within the adsorbent bed to get the response without adsorption. The adsorbent bed downstream analysis was performed with a mass spectrometer (Hiden Analytical HPR

20 QIC). A complete description of the adsorption setup is available elsewhere. (Baur et al. 2015a).

A standard adsorption capacity measurement consisted of the following steps:

1. Stabilization of formaldehyde mixture flow through the bypass for 15 min to measure the initial formaldehyde concentration.
2. After a switch to the reactor, the formaldehyde mixture flowed through the adsorbent bed until the continuously measured outlet formaldehyde concentration reached its initial value measured during the stabilization step.

In such a manner a breakthrough curve was obtained. The breakthrough curves were numerically integrated and the adsorption capacities for all samples were calculated.

### 2.4 Temperature-programmed desorption (TPD)

TPD was carried out in the same experimental setup with ACF/20%DETA. The samples was heated in a He flow ( $50 \text{ cm}^3 \cdot \text{min}^{-1}$ ) at  $10 \text{ K} \cdot \text{min}^{-1}$ . The gas leaving the reactor was continuously monitored by the mass spectrometer (mass 18 and 44) and plotted as a function of temperature to obtain a TPD pattern.

## 3 Results and discussion

A representative SEM picture of original ACFs material is shown in Fig. 1. The elementary filaments forming the ACFs network have a diameter around  $10 \mu\text{m}$ . Their relative small diameter enhances the adsorption kinetics by reducing the mass transfer limitations (between the outer surface and the active sites for adsorption inside the pores). Moreover, such thin filaments render the macrostructure of the ACFs very open, avoiding high pressure drop at fast gas passage during adsorption process. Hence, ACFs adsorbent bed allows

a higher gas throughput as compared to a bed composed of granular adsorbents such as activated carbon, zeolite or silica. The general aspect of the ACFs samples did not change upon the different DETA loadings.

The morphology of different samples was studied via  $\text{N}_2$  adsorption isotherms which are shown in Fig. 2 for original and DETA modified ACFs. As can be seen the largest micropore volume is measured for the original ACFs. The  $\text{N}_2$  adsorption isotherms of the DETA functionalized samples indicate a smaller pore volume suggesting that DETA is filling the fiber's pores. All the recorded isotherms are characterized by a steep slope at low  $\text{N}_2$  partial pressure followed by an almost flat curve until the saturation. Such adsorption isotherms correspond to the type I according to the IUPAC classification, indicating a microporous structure (pore diameter  $> 2 \text{ nm}$ ) (Sing et al. 1985). Moreover, all the analyzed samples showed a slope change at the same  $\text{N}_2$  partial pressure suggesting a constant loading mean micropore diameter, independently of the DETA loading. The specific

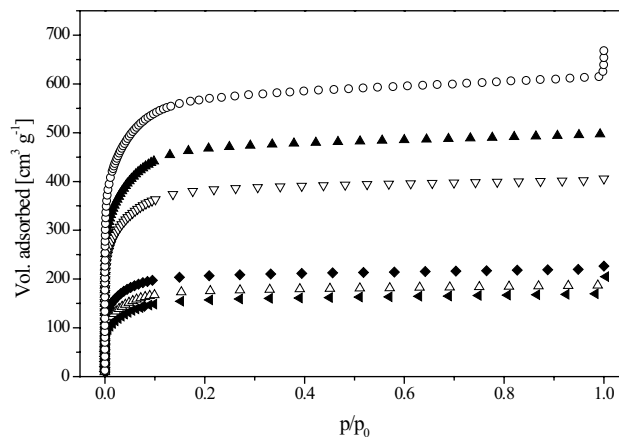


Fig. 2  $\text{N}_2$  adsorption isotherms (77 K) for ACF (open circle), ACF/5%DETA (filled triangle), ACF/15%DETA (inverted open triangle), ACF/20%DETA (filled diamond), ACF/25%DETA (open triangle) and ACF/35%DETA (left pointing triangle)

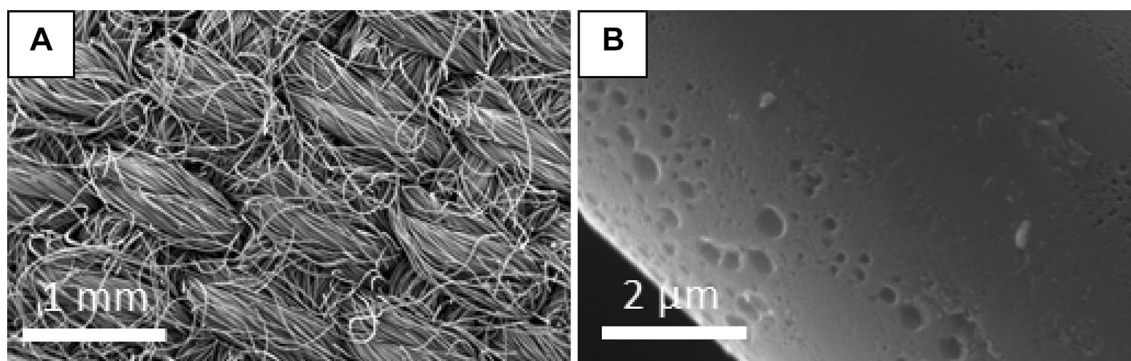
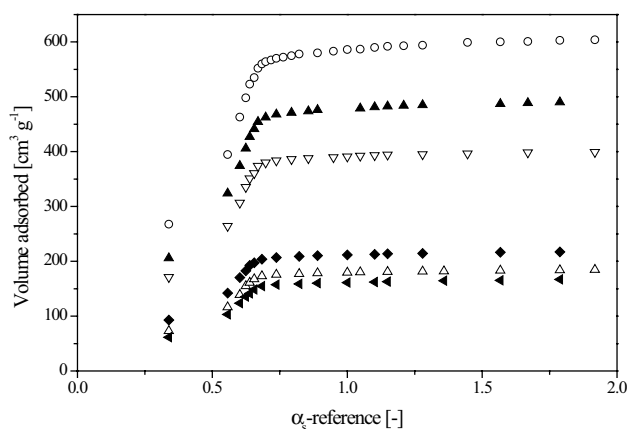


Fig. 1 SEM image of activated carbon fibers (ACFs) with a small (a) and large (b) magnification

surface area of the adsorbent was calculated from  $N_2$  adsorption data using the BET equation linearized in the pressure range from 0.01 to 0.1 for all the samples.

A deeper insight on the microstructure is obtained by comparing the  $\alpha_s$ -plot of the different samples. The  $\alpha_s$ -plot is based on the comparison of the  $N_2$  adsorption isotherms between a porous adsorbent and a chemically similar non-porous reference material. The  $\alpha_s$ -reference is obtained by normalizing the amount of  $N_2$  adsorbed onto the non-porous reference at different partial pressures by the amount adsorbed at  $p/p_0=0.4$ . The amount of  $N_2$  adsorbed on the surface of the studied adsorbent is then plotted against the  $\alpha_s$  reference at the corresponding partial pressure. In this study, carbon black was used as non-porous reference material ( $SSA=9\text{ m}^2\cdot\text{g}^{-1}$ ). The  $\alpha_s$ -plot of all samples is shown in Fig. 3. For all the samples at low  $\alpha_s$  the curve is relatively steep whereas at  $\alpha_s > 1$  the curves are linear and almost constant. Such curves are typically assigned to microporous material. The steepness of the curve at low  $\alpha_s$  reference indicates that most of the surface is confined in the porosity whereas the flatness of the curve at high  $\alpha_s$  values is the characteristic of a relatively small external surface area as compared to the total surface. It is worth noticing that regardless of the DETA loading, the slope change occurs at the same  $\alpha_s$ -reference confirming a constant pore width. So, we conclude that the DETA deposition does not reduce the pore width. This situation is in line with the pores filled gradually from the swage bottom of the micropores.

As summarized in Table 1, the pore volume decreases drastically with the DETA loading up to 20 wt.% DETA whereas at higher loading (26 and 35 wt.%) the decrease of the pore volume is less pronounced. This phenomenon along with the constant micropore size upon DETA loading (showed by the analysis of the  $\alpha_s$ -plot) suggests a micropore



**Fig. 3**  $\alpha_s$ -plot for ACF (open circle), ACF/5%DETA (filled triangle), ACF/15%DETA (inverted open triangle), ACF/20%DETA (filled diamond), ACF/25%DETA (open triangle) and ACF/35%DETA (left pointing triangle)

**Table 1** Influence of the DETA loading on the specific surface area (SSA) and the pore volume of the adsorbent

Sample	$SSA_{BET}$ ( $\text{m}^2\text{ g}^{-1}$ )	$C$	Micropore volume ( $\text{cm}^3\text{ g}^{-1}$ )
ACF	$2170 \pm 50$	280	$0.94 \pm 0.02$
ACF/5% DETA	$1760 \pm 50$	360	$0.74 \pm 0.02$
ACF/15% DETA	$1460 \pm 50$	280	$0.64 \pm 0.02$
ACF/20% DETA	$810 \pm 30$	260	$0.34 \pm 0.02$
ACF/26% DETA	$680 \pm 30$	240	$0.27 \pm 0.02$
ACF/35% DETA	$610 \pm 30$	215	$0.26 \pm 0.02$

filling and not a layer by layer deposition of DETA. A layer by layer deposition of DETA is difficult to expect since DETA is deposited via wetness impregnation by ethanol solution followed by ethanol vaporization. Since only the pore volume was found to decrease and assuming slit-shaped micropores as often reported for ACFs (Kaneko et al. 1992), we suggest that their bottom has a swage form and is gradually filled from the bottom to the top with DETA. With the assumption of an ideal filling of the micropores and the value of the liquid density of DETA it is possible to calculate the pore volume remaining after DETA deposition. Such volume should correspond to the micropore volume measured with  $N_2$  isotherms.

With the liquid density of DETA being  $0.995\text{ g cm}^{-3}$ , a sample containing 20 wt.% of DETA should have a reduction of the micropore volume of  $0.2\text{ cm}^{-3}$ . The micropore volume of original ACFs being  $0.94\text{ cm}^3\text{ g}^{-1}$ , ACFs with 20 wt.% DETA should show a total micropore volume of  $0.74\text{ cm}^3\text{ g}^{-1}$ , whereas the  $N_2$  adsorption measurements showed only  $0.34\text{ cm}^3\text{ g}^{-1}$ . This large difference ( $0.4\text{ cm}^3\text{ g}^{-1}$ ) is explained by specific place of DETA within the micropores. The molecular size of DETA is estimated at around  $10\text{ \AA}$  based on molecular drawing. Hence, due to its intrinsic size and small mean diameter ( $\sim 2\text{ nm}$ ) of slit-shape micropores, we suggest that DETA is blocking partially the micropores. A part of the micropore volume is then hindered by DETA and is not available for  $N_2$  adsorption explaining the large difference between the measured and theoretical micropore volume. Closer to the surface, the micropore diameter becomes larger and DETA can occupy the volume more efficiently. Hence, the difference of micropore volume between ACFs/20% DETA and ACFs/26% DETA is only of  $0.07\text{ cm}^3\text{ g}^{-1}$ , reaching the theoretical value of  $0.06\text{ cm}^3\text{ g}^{-1}$ .

The analysis of the SSA upon DETA loading also confirms the hypothesis of a partial loss of the micropore volume due to spatial limitation (Table 1). The SSA of the DETA treated samples is also decreasing drastically at DETA loading up to 20 wt.% whereas at higher loading the decrease is less pronounced. Similarly to the pore volume a large portion of the SSA of the original ACFs



becomes unavailable for N<sub>2</sub> due to the coverage by DETA. It is important to underline that the DETA deposition does not influence the C value of the BET equation (an indicative parameter of the adsorption energies) confirming a constant pore width and supporting our speculation about the pore filling by DETA.

A schematic representation of the DETA deposition in slit-shaped micropore with swage type lower part is shown in Fig. 4 based on the evolution of the micropore volume, the SSA and the mean pore width. In conclusions, based on the analysis of the micropore volume, the SSA and the pore width, the optimum DETA loading is around 15–20 wt.% for the ACFs used in this study.

Formaldehyde adsorption (50 ppmv) over original and DETA (5%) modified ACFs is shown in Fig. 5. The concentrations of formaldehyde and argon are normalized for the sake of comparison. As can be seen the breakthrough curve of original ACFs occurs extremely quickly implying a very small adsorption capacity (0.1 wt.%) being in line with the performance reported in the literature for similar adsorbents. (Tanada et al. 1999; Song et al. 2007) The deposition of 5% DETA on the fibers leads to a large increase (25-fold) of the formaldehyde abatement (2.5 wt.%). Before reaching the value of the injected concentration, the formaldehyde signal detected by the mass spectrometer after the adsorption bed remains at zero during 15 min indicating a total formaldehyde removal. Moreover, the relative steepness of the breakthrough curve suggests fast adsorption kinetics. In comparison to both formaldehyde breakthrough curves, the argon curves raise extremely quickly underlying the very fast time of passage of the gas through the adsorbent bed.

The large increase of the adsorption capacity noticed for ACFs/5%DETA as compared to original fibers despite the reduction of both SSA and micropore volume (Table 1)

Fig. 4 Schematic representation of micropore filling by DETA

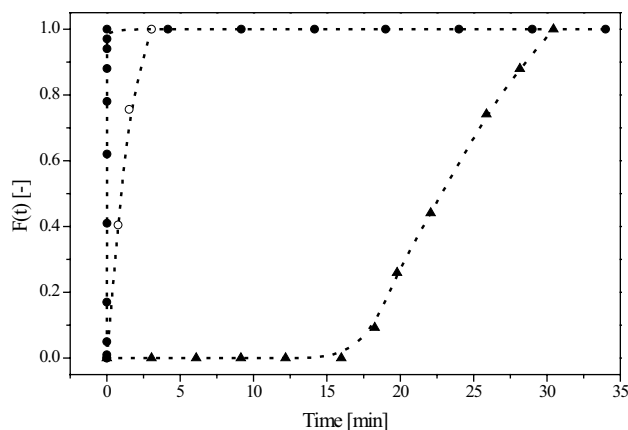
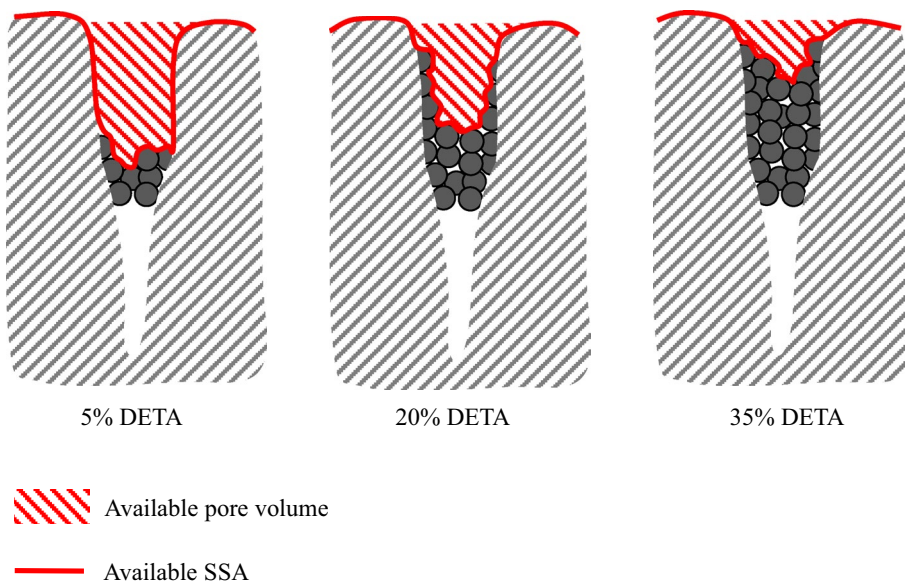


Fig. 5 Formaldehyde (50 ppmv) breakthrough curves for ACF (open circle), ACF/5% DETA (filled triangle) and 2% (v/v) Argon (filled circle). Total flow rate (STP) 300 cm<sup>3</sup> min<sup>-1</sup> (298 K)

suggests that the intrinsic microporosity of the ACFs is not sufficient for the adsorption of formaldehyde. Such observation was already reported for polar VOCs (Baur et al. 2015a) whereas for non-polar VOC adsorption the morphology was found to be of primary importance (Lillo-Rodenas et al. 2011, 2005; Baur et al. 2015c). However, high porosity of the carbon fibers offers a large surface for the homogeneous deposition of DETA leading to the high amount of adsorption sites. In this way a large amount of the sites specific for formaldehyde adsorption are created.

DETA is an organic high boiling point molecule (477 K) containing three amine groups and can therefore increase the formaldehyde removal via chemical interactions as compared to non-functionalized ACFs. Moreover, due to its low volatility, evaporation of DETA from the ACFs is avoided at room temperature. We suggest that the amine groups are

active for the formaldehyde adsorption. The importance of amine groups was already reported for the removal of aldehydes. Matsuo et al. suggested a Schiff base interaction between the aldehyde and the electron rich nitrogen atom of the amine group as the adsorption mechanism (Matsuo et al. 2008). Such type of adsorption is called chemisorption. Chemisorption is particularly powerful for low boiling points VOCs and was already reported for other type of surface functionalization (Baur et al. 2015b). Although chemisorption is supposed to create stronger adsorbent-adsorbate interactions, in this system only interactions between formaldehyde and DETA are supposed. The strength of these interactions remains unknown.

To get a deeper understanding of the importance of the Schiff base mechanism, the treated ACFs were heated at 673 K under a helium gas flow. As shown on Fig. 6, a peak of CO<sub>2</sub> occurs below 373 K. We attribute the presence of CO<sub>2</sub> to the capture of ambient CO<sub>2</sub> by the ACFs adsorbents during storage since amine groups are relatively basic and well known to interact with CO<sub>2</sub> (Couck et al. 2009). These interactions are sometimes used for CO<sub>2</sub> storage (D'Alessandro et al. 2010). The desorption peak of H<sub>2</sub>O occurring between 373 and 673 K is attributed to a chemical reaction between the amines groups and the oxygen containing groups present on the surface of the carbon fibers. These O-containing groups are of different type (carboxylic, ketones...) but are present at relatively high concentration (Figueiredo et al. 1999). We suggest a reaction between the amine groups and the oxygen contained groups on the ACFs surface forming an amide. During this reaction a water molecule is produced and appears as a TPD peak. To confirm the

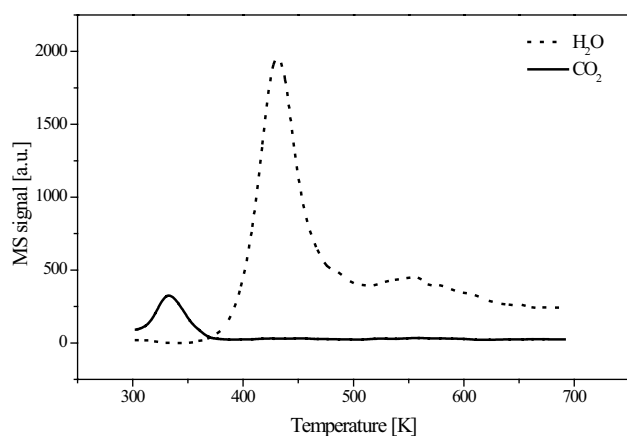


**Fig. 6** TPD profile of ACF/20%DETA (10 K min<sup>-1</sup>, 50 cm<sup>3</sup> min<sup>-1</sup>). The solid line describes the CO<sub>2</sub> desorption curve with a small desorption peak at low temperature attributed to physisorbed CO<sub>2</sub>. The dashed line represents the emission of H<sub>2</sub>O from the adsorbent. The peaks at 440 K and 550 K are attributed to the reaction of the amine group of DETA with two types of O-containing groups of the ACF surface. The TPD did not show signal of any other species in the gas phase

importance of the Schiff base mechanism, adsorption of formaldehyde has been carried out over the ACFs with DETA heated at 673 K in He (to deactivate the amine groups). Such adsorbent (supposed to have only amides) showed a considerably lower adsorption capacity demonstrating the necessity of the amines groups for formaldehyde removal. The chemisorption of formaldehyde on amine groups via a Schiff base mechanism is therefore highly probable. Based on this observation we also concluded that DETA deposited via wetness impregnation is physisorbed on the surface of the ACFs. The heating process leads to chemisorption of DETA on the ACFs samples. Such chemical interaction deactivates a part of the sites for formaldehyde chemisorption.

To increase the formaldehyde abatement capacity of the ACFs, the loading of DETA was varied as shown in Fig. 7. The increase of the DETA loading enhances linearly the formaldehyde adsorption capacity (loading < 20 wt.%) up to a maximum value of 8.6 wt.%. For all DETA loadings the formaldehyde signal at the reactor outlet reached zero insuring a total removal from the gas stream. As depicted in Fig. 7, further increase of the DETA loading leads to a slight decrease of the adsorption capacity. This phenomenon was already reported for hexamethylene diamine deposition on activated carbon (Ma et al. 2011) and was explained by the pore volume decrease at high loading. Hence, the optimum DETA loading for ACF used in this study is around 20 wt.%.

The important decrease of the SSA and the micropore volume was also noticed to occur at 20 wt.% loading of DETA (Table 1). Therefore, we suggest that the surface covered with amine adsorption sites is maximized at this loading. Further increase of the DETA loading is decreasing the adsorption capacity indicating that not all DETA functional groups are involved in formaldehyde adsorption. Such observation along with the DETA pore filling suggested in Fig. 4 is another indication of the adsorption mechanism. We

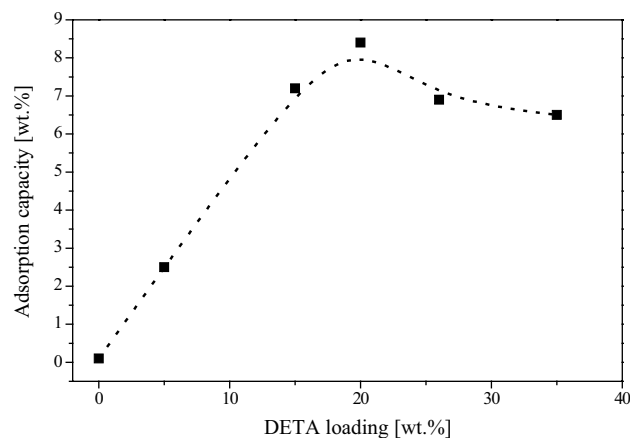


**Fig. 7** Influence of the DETA loading on the formaldehyde (50 ppmv) removal capacity (298 K)

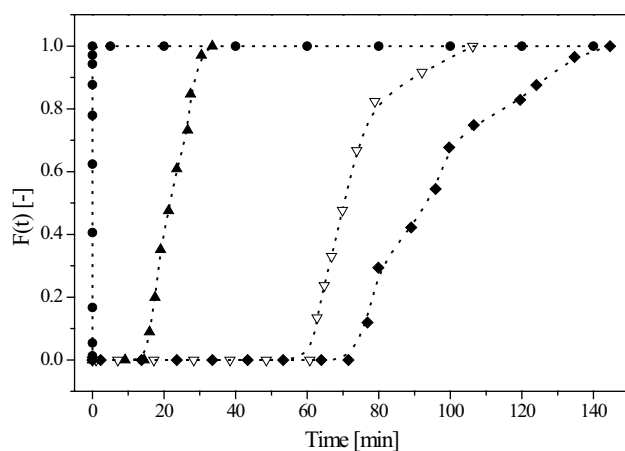


**Fig. 8** Formaldehyde (50 ppmv) breakthrough curves for ACF/5% DETA (filled triangle) ACF/15% DETA (inverted open triangle), ACF/20%DETA (filled circle) and 2% (v/v) Argon (filled circle); Total flow rate (STP)  $300 \text{ cm}^3 \cdot \text{min}^{-1}$  (298 K)

suggest that the optimum formaldehyde adsorption capacity is reached once the surface of the fibers covered with amine groups is the largest. At low DETA loading the surface covered with amine is also low leading to a small adsorption capacity. This surface can be further increased while depositing more DETA with a maximum at 20 wt.%. The pores are partially filled and part of the DETA is also deposited on the pore walls increasing considerably the amine groups available for interactions with formaldehyde. A further addition of DETA fills more micropores but decreases the amine available surface and so decreases slightly the adsorption capacity.

In order to get a deeper insight on the adsorption dynamic, the breakthrough curves of ACFs/5% DETA, ACFs/15%DETA and ACFs/20%DETA are plotted in Fig. 8. ACFs/5% DETA shows the steepest breakthrough curve whereas for higher loading the shape is less sharp. The steepness of the breakthrough curve indicates the kinetics of the adsorption. A steep breakthrough curve allows suggesting fast adsorption kinetics (low mass transfer limitations) whereas higher mass transfer limitations result in less steep breakthrough curve. The mass transfer limitations during the adsorption seem to increase with the DETA loading.

In the adsorbent with low DETA loading (5 wt.%) the adsorption kinetics is very fast implying that formaldehyde reaches the adsorption sites quasi-instantaneously. On the opposite, at higher loading, the breakthrough curve clearly presents a two steps adsorption mechanism illustrated by the two distinct slopes on the breakthrough curve. The first adsorption step is characterized by a relatively steep breakthrough curve followed by a second step where the curve shows a flatter profile. We suggest that the first step occurs similarly to low DETA loading adsorbent with fast

interaction between formaldehyde and the adsorption site. During the second slower step formaldehyde molecules diffuse to the sites inside the DETA layer in the pore bottom.

The adsorption kinetics obtained from the analysis of breakthrough curve could also suggest the adsorbent morphology. As explained earlier, DETA molecules give the unique adsorption sites for formaldehyde in the synthesized adsorbents. The disposition of DETA in the micropores governs then directly the kinetic of adsorption. The fast adsorption kinetic at low loading suggests easy access of formaldehyde to the adsorption site. The location of DETA at the middle of the micropore suggested by the analysis of the pore volume is confirmed by the adsorption kinetics observed by ACFs/5%DETA. In the case of higher loadings (ACFs/20%DETA), the first quick adsorption step indicates the presence of adsorption sites with high accessibility. Hence, in accordance with the  $\text{N}_2$  analysis and the increased adsorption capacity we suggest that DETA is partially disposed on the side of the micropores as well as in the bottom. At the beginning of the adsorption the formaldehyde is adsorbed on the adsorption sites located on the side of the micropores (1st step) while hindering the sites at the bottom. During the 2nd step formaldehyde migrates to the adsorption sites located at the bottom of the micropores. The morphology of ACFs modified by DETA as follows from the analysis of the SSA, the measured and theoretical pore volume is consistent with the analysis of the adsorption kinetics.

## 4 Conclusions

In summary, efficient structured adsorbent was developed for the formaldehyde removal at low concentration in air by deposition of s DETA on the surface of microporous activated carbon fibers (ACFs). Adsorbents with different DETA loading were synthesized and characterized. Morphology of ACFs with the surface covered by DETA was suggested based on the analysis of change with DETA loading of specific surface area and microporosity.

At optimum DETA loading of 20 wt.%, ~100-fold increase of adsorption capacity as compared to original ACFs was achieved. A Schiff base reaction between the amine groups of DETA and formaldehyde was suggested as the adsorption mechanism. In general, the presence of basic functional groups on activated carbon surface enhances the formaldehyde adsorption. The surface chemistry is more important than the microporous structure for efficient formaldehyde removal.

**Acknowledgements** The authors acknowledge Swiss Federal Institute of technology in Lausanne (EPFL) and the Russian Science Foundation (Grant 15-19-20023) for funding the research presented in this manuscript.

## References

- Baur, G.B., Beswick, O., Spring, J., Yuranov, I., Kiwi-Minsker, L.: Activated carbon fibers for efficient VOC removal from diluted streams: the role of surface functionalities. *Adsorpt. J. Int. Adsorpt. Soc.* **21**(4), 255–264 (2015a)
- Baur, G.B., Yuranov, I., Kiwi-Minsker, L.: Activated carbon fibers modified by metal oxide as effective structured adsorbents for acetaldehyde. *Catal. Today* **249**, 252–258 (2015b)
- Baur, G.B., Yuranov, I., Renken, A., Kiwi-Minsker, L.: Activated carbon fibers for efficient VOC removal from diluted streams: the role of surface morphology. *Adsorpt. J. Int. Adsorpt. Soc.* **21**(6–7), 479–488 (2015c)
- Boonmuayvitaya, V., Sae-ung, S., Tanthapanichakoon, W.: Preparation of activated carbons from coffee residue for the adsorption of formaldehyde. *Sep. Purif. Technol.* **42**(2), 159–168 (2005)
- Carter, E.M., Katz, L.E., Speitel, G.E., Ramirez, D.: Gas-phase formaldehyde adsorption isotherm studies on activated carbon: correlations of adsorption capacity to surface functional group density. *Environ. Sci. Technol.* **45**(15), 6498–6503 (2011)
- Couck, S., Denayer, J.F.M., Baron, G.V., Remy, T., Gascon, J., Kapteijn, F.: An amine-functionalized MIL-53 metal-organic framework with large separation power for CO<sub>2</sub> and CH<sub>4</sub>. *J. Am. Chem. Soc.* **131**(18), 6326–6326+ (2009)
- D'Alessandro, D.M., Smit, B., Long, J.R.: Carbon dioxide capture: prospects for new materials. *Angew. Chem. Int. Edit.* **49**(35), 6058–6082 (2010)
- Ewlad-Ahmed, A.M., Morris, M.A., Patwardhan, S.V., Gibson, L.T.: Removal of formaldehyde from air using functionalized silica supports. *Environ. Sci. Technol.* **46**(24), 13354–13360 (2012)
- Figueiredo, J.L., Pereira, M.F.R., Freitas, M.M.A., Orfao, J.J.M.: Modification of the surface chemistry of activated carbons. *Carbon* **37**(9), 1379–1389 (1999)
- Hauptmann, M., Lubin, J.H., Stewart, P.A., Hayes, R.B., Blair, A.: Mortality from solid cancers among workers in formaldehyde industries. *Am. J. Epidemiol.* **159**(12), 1117–1130 (2004)
- Kaneko, K., Shimizu, K., Suzuki, T.: Intrapore field-dependent micropore filling of supercritical N<sub>2</sub> in slit-shaped micropores. *J. Chem. Phys.* **97**(11), 8705–8711 (1992)
- Kim, D.I., Park, J.H., Kim, S.D., Lee, J.Y., Yim, J.H., Jeon, J.K., Park, S.H., Park, Y.K.: Comparison of removal ability of indoor formaldehyde over different materials functionalized with various amine groups. *J. Ind. Eng. Chem.* **17**(1), 1–5 (2011)
- Lee, K.J., Miyawaki, J., Shiratori, N., Yoon, S.H., Jang, J.: Toward an effective adsorbent for polar pollutants: formaldehyde adsorption by activated carbon. *J. Hazard. Mater.* **260**, 82–88 (2013)
- Lillo-Rodenas, M.A., Cazorla-Amoros, D., Linares-Solano, A.: Behaviour of activated carbons with different pore size distributions and surface oxygen groups for benzene and toluene adsorption at low concentrations. *Carbon* **43**(8), 1758–1767 (2005)
- Lillo-Rodenas, M.A., Cazorla-Amoros, D., Linares-Solano, A.: Benzene and toluene adsorption at low concentration on activated carbon fibres. *Adsorpt. J. Int. Adsorpt. Soc.* **17**(3), 473–481 (2011)
- Ma, C.J., Li, X.H., Zhu, T.L.: Removal of low-concentration formaldehyde in air by adsorption on activated carbon modified by hexamethylene diamine. *Carbon* **49**(8), 2873–2875 (2011)
- Matsuo, Y., Nishino, Y., Fukutsuka, T., Sugie, Y.: Removal of formaldehyde from gas phase by silylated graphite oxide containing amino groups. *Carbon* **46**(8), 1162–1163 (2008)
- Obuskovic, G., Majumdar, S., Sirkar, K.K.: Highly VOC-selective hollow fiber membranes for separation by vapor permeation. *J. Membr. Sci.* **217**(1–2), 99–116 (2003)
- Pei, J.J., Zhang, J.S.S.: On the performance and mechanisms of formaldehyde removal by chemi-sorbents. *Chem. Eng. J.* **167**(1), 59–66 (2011)
- Rong, H.Q., Ryu, Z.Y., Zheng, J.T., Zhang, Y.L.: Influence of heat treatment of rayon-based activated carbon fibers on the adsorption of formaldehyde. *J. Colloid Interface Sci.* **261**(2), 207–212 (2003)
- Sing, K.S.W., Everett, D.H., Haul, R.A.W., Moscou, L., Pierotti, R.A., Rouquerol, J., Siemieniowska, T.: Reporting physisorption data for gas solid systems with special reference to the determination of surface-area and porosity (recommendations 1984). *Pure Appl. Chem.* **57**(4), 603–619 (1985)
- Singh, K.P., Mohan, D., Tandon, G.S., Gupta, G.S.D.: Vapor-phase adsorption of hexane and benzene on activated carbon fabric cloth: equilibria and rate studies. *Ind. Eng. Chem. Res.* **41**(10), 2480–2486 (2002)
- Song, Y., Qiao, W., Yoon, S.H., Mochida, I., Guo, Q., Liu, L.: Removal of formaldehyde at low concentration using various activated carbon fibers. *J. Appl. Polym. Sci.* **106**(4), 2151–2157 (2007)
- Tanada, S., Kawasaki, N., Nakamura, T., Araki, M., Isomura, M.: Removal of formaldehyde by activated carbons containing amino groups. *J. Colloid Interface Sci.* **214**(1), 106–108 (1999)
- W.H.O.: Air quality guidelines for Europe, 2nd edn., pp. 87–91. World Health Organization, Regional Office for Europe, Copenhagen (2000)